

We would like to thank the anonymous reviewer for the comments that significantly improved the clarity and readability of the manuscript. Our point-by-point responses are found below in blue ink. The revised content is highlighted in yellow.

General Comments:

The normalization and portability of atmospheric pollutant monitoring are crucial for in-depth research into local variations in atmospheric environment and pollution. This manuscript establishes a low-cost air quality monitoring device and applies it to estimate the hygroscopicity parameters of aerosols, comparing the results with site observation data. The study holds certain scientific and application value and aligns with the publication scope of the Atmospheric Measurement Techniques journal. However, there are some scientific and technical issues within the manuscript itself, suggesting major revisions before reconsidered.

Specific Comments:

1) The accuracy and error range of AQB in detecting aerosols and the application of AQB to estimate aerosol hygroscopicity parameters should be two separate research components with a sequential order. However, in this manuscript, the authors often fail to clearly distinguish between the two. The authors adopt a method of setting RH thresholds to classify AQB observation results into dry aerosols and humidified aerosols, and then compares and calibrates the observations of dry aerosols with EPA station data, which is a feasible approach. However, in Sections 3.1, 3.2, and Figures 2 and 3, the authors do not classify or analyze the data based on the RH threshold set by themselves. Meanwhile, as shown in Figure 2(b), the occurrence of RH below 50% during the observation period is rare. Can such a limited amount of data support the examination of the reliability of AQB detection?

A: We appreciate the reviewer's insightful comments. In response to concerns, Fig R1, similar in configuration to Figs. 3(a-c), shows the data points at  $RH \leq 50\%$ , which were applied to determine the sensitivity coefficient ( $\alpha$ ).

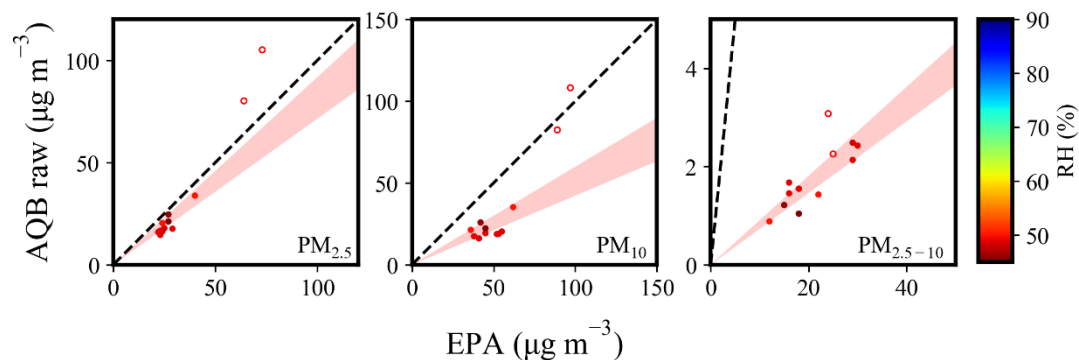


Figure R1. The correlation of mass concentration between TW-EPA and OPC in AQB #1 (raw data) for PM<sub>2.5</sub>, PM<sub>10</sub>, and PM<sub>2.5-10</sub> at  $RH \leq 50\%$ . The hollow points are the two significant outliers mentioned in Table 2.

Although these data points constitute about 5% of the total (i.e., 17 out of 356 points), a high correlation between the AQB and TW-EPA measurements was observed. Figure 2(b) shows only part of the campaign to reveal the temporal comparison between AQB and TW-EPA data. As stated in section 2.3, the statistical distribution of  $M_{EPA}$  to  $M_{OPC}$  ratios at  $RH \leq 50\%$  was analyzed to evaluate a sensitivity coefficient ( $\alpha$ ) as the mean value  $\pm 0.5\sigma$  ( $\sigma$ : standard deviation). The shaded area in Fig. R1 represents the distribution of  $\alpha$ , covering most of the data points at  $RH \leq 50\%$ . The same calculation but for higher RH thresholds (up to 60% to have more data points, 51 out of 356) summarized below shows a similar  $\alpha$  range, indicating sufficient data points at  $RH \leq 50\%$  for a conclusive  $\alpha$ . The following figure is added to the supplementary as Fig. S2 to clarify this issue. In the content, Lines 179-181 were revised as follows: “The estimated  $\alpha$ , as summarized in Table 1, are higher for  $PM_{10}$  than for  $PM_{2.5}$ , i.e.,  $2.02 \pm 0.34$  vs  $1.26 \pm 0.16$ , which are reasonably conclusive as tested with more data points selected at higher RH thresholds (Fig. S2).”

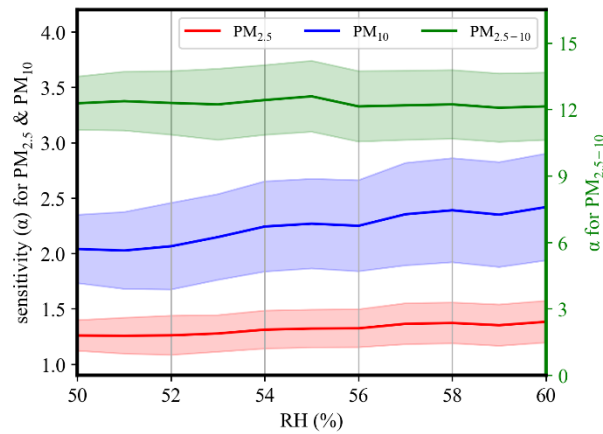


Figure S2: The determined sensitivity as a function of RH thresholds for  $PM_{2.5}$  (red),  $PM_{10}$  (blue) and  $PM_{2.5-10}$  (green). The shading area is the mean value  $\pm 0.5\sigma$

As to the accuracy of applied methods, the comparison analysis between fitted data and TW-EPA data is summarized in a new table (Table 2) added to the content as follows:

Table 2: Performance metrics of different calibration methods for  $PM_{2.5}$ ,  $PM_{2.5-10}$ , and  $PM_{10}$ .

	$PM_{2.5}$			$PM_{2.5-10}$			$PM_{10}$			
	RH $\leq$ 50% Only <sup>a</sup>	All data (no $\kappa$ )	All data ( $\kappa=0.29$ )	RH $\leq$ 50% Only <sup>a</sup>	All data (no $\kappa$ )	All data ( $\kappa=0.09$ )	RH $\leq$ 50% Only <sup>a</sup>	All data (no $\kappa$ )	All data ( $\kappa=0.36$ )	( $PM_{2.5}+PM_{2.5-10}$ ) <sup>c</sup>
applied $\alpha$	1.26 $\pm$ 0.16	1.04	1.40	12.37 $\pm$ 1.33	10.77	13.16	2.02 $\pm$ 0.34	1.69	2.36	—
MAPE (%)	21.3 (12.8)	48.8	24.8	15.9 (11.5)	37.9	31.8	32.8 (18.5)	62.5	29.2	18.2
RMSE ( $\mu\text{g cm}^{-3}$ )	20.5 (3.7)	29.1	11.3	4.9 (2.8)	9.4	9.1	42.6 (10.3)	54.7	26.9	15.9
$R^2$ <sup>b</sup>	0.55 (0.51)	-3.49	0.32	0.31 (0.78)	0.57	0.59	-4.18 (-0.58)	-4.74	-0.38	0.51

<sup>a</sup> Only for data points at  $RH \leq 50\%$ . The value in parentheses is the performance result without two significant outliers shown in Fig. 3

<sup>b</sup> Coefficient of determination ( $R^2$ ) is calculated as the proportion of variation in the calibrated dry mass concentration.

<sup>c</sup> The combination of calibrated data from  $PM_{2.5}$  All data ( $\kappa=0.29$ ) and  $PM_{2.5-10}$  All data ( $\kappa=0.09$ ).

The MAPE and RMSE for  $RH \leq 50\%$  are 12.8% and  $3.7 \mu\text{g cm}^{-3}$  for  $\text{PM}_{2.5}$ , 11.5% and  $2.8 \mu\text{g cm}^{-3}$  for  $\text{PM}_{2.5-10}$ , without considering the two significant outliers. The performance of AQB for  $\text{PM}_{2.5}$  and  $\text{PM}_{10}$  through different calibration methods was discussed in Section 3.2 (Lines 172-211) as “Figures 3(a) and 3(c) show the scatter distribution of the mass concentrations between AQB #1 (with no calibration) and TW-EPA data for  $\text{PM}_{2.5}$  and  $\text{PM}_{10}$ , respectively. Overall, the PM mass concentrations measured by AQB system appear to be higher than those reported by TW-EPA. The results reveal an apparent influence of ambient RH, indicating the contribution of water content. The red-shaded area represents a regression line with a slope corresponding to the inverse of the sensitivity coefficients ( $\alpha$ ) derived from data points at ambient  $RH \leq 50\%$  (17 out of 356 points, 5%). The notable deviation of the red shaded area from the 1:1 line towards the right side indicates the requirement of  $\alpha > 1$  corrections, contributed by the different measurement principles and calibration techniques, which may result from the assuming particle density and refractive index (RI) (dust, density:  $1.65 \text{ g cm}^{-3}$ , RI:  $1.5 + 0i$ ). The estimated  $\alpha$ , as summarized in Table 1, are higher for  $\text{PM}_{10}$  than for  $\text{PM}_{2.5}$ , i.e.,  $2.02 \pm 0.34$  vs  $1.26 \pm 0.16$ , which are reasonably conclusive as tested with more data points selected at higher RH thresholds (Fig. S2). The  $\alpha$  difference between  $\text{PM}_{2.5}$  and  $\text{PM}_{10}$  might be attributed to the complex composition of ambient particles, which differs from the samples used for instrument calibration, as well as possible sensitivity variations in OPC over time. With sensitivity calibration, the performance at ambient  $RH \leq 50\%$  exhibits a strong correlation with MAPE at 12.8%, 18.5%, and Root Mean Squared Error (RMSE) at  $3.7 \mu\text{g m}^{-3}$ ,  $10.3 \mu\text{g m}^{-3}$  for  $\text{PM}_{2.5}$  and  $\text{PM}_{10}$ , respectively, as summarized in Table 2 excluding the two significant outliers (shown as hollow circles in Fig. 3). The results confirm the effectiveness of OPCs in capturing PM concentrations, consistent with previous real-time outdoor field studies (Gillooly et al., 2019; Demanega et al., 2021; Sá et al., 2022; Crilley et al., 2018). Additionally, the OPC sampling flow rate has an impact on measurement performance. AQB #1 maintained a steady rate at  $3.6 \pm 0.2 \text{ LPM}$ , whereas AQB #2 exhibits two distinct time periods with sampling flow rates of 3.6-4.2 LPM for the first period and 3.2-3.6 LPM for the second period. ... With the derived  $\alpha$ , the hygroscopicities were retrieved using Eq. (3), resulting in  $\kappa$  ranging from 0.18 to 0.29 for  $\text{PM}_{2.5}$  and 0.20 to 0.39 for  $\text{PM}_{10}$  (Table 1) during the studied period. Figures 3(d) and 3(f) show the scatter distribution of the derived dry concentration vs. TW-EPA concentration for  $\text{PM}_{2.5}$  and  $\text{PM}_{10}$ , respectively. The results from the two AQB systems exhibit slight differences but are consistent overall. Considering both the sensitivity coefficient and hygroscopicity, the performance of AQB in deriving dry PM concentration is significantly improved with lower MAPE, RMSE, and higher  $R^2$  than the results obtained using only the sensitivity coefficient, as summarized in Table 2. ... The lower  $\kappa$  for  $\text{PM}_{2.5-10}$  might suggest a significant contribution from dust or other less hygroscopic species, consistent with the IC analyses in Table 3 and discussed further in Sect. 3.3. With the retrieved  $\alpha$  and  $\kappa$  for  $\text{PM}_{2.5}$  and  $\text{PM}_{2.5-10}$ , Fig. 3(e) shows the scatter distribution between the derived dry  $\text{PM}_{2.5-10}$  from AQB data and TW-EPA data, exhibiting a MAPE of 31.8%, more significant than the 24.8% for  $\text{PM}_{2.5}$ . ... Detection efficiency may be influenced by notable spatial variations, aligning with the findings of Kaliszewski et al. (2020), which showed a reduced correlation between OPC-N3 measurements and reference instruments for larger particles. The dry  $\text{PM}_{10}$  derived from AQB through the divided  $\text{PM}_{2.5}$  and  $\text{PM}_{2.5-10}$  analysis demonstrates better consistency with the reported TW-EPA data than the direct calibration method. This is evidenced by a lower

MAPE in Fig. 3(g) (18.2%) compared to Fig. 3(f) (29.2%) and a significant improvement than the simple linear regression method, which has a higher MAPE at 62.5% (Table 2). This substantiates the importance of considering composition heterogeneity among particle sizes for accurate dry PM derivation.”.

2) Introducing aerosol chemical composition observations into a thermodynamic equilibrium model to calculate aerosol hygroscopic growth and comparing it with optical observations is a common research approach. However, contrasting different field experiments conducted at different times (with an 8-year difference) and different underlying surfaces by the authors doesn't have much significance.

A: Thank you for highlighting the concerns regarding the comparison of derived hygroscopicity between two different field studies conducted in different years. We acknowledge that the hygroscopic characteristics of ambient particles can vary spatially and temporally. Our comparison of the chemical composition of PM<sub>2.5</sub> from two winter sampling campaigns in 2013 and 2021 revealed that the composition concentration might be different, but the derived hygroscopicity was consistent across these years, demonstrating typical ambient PM<sub>2.5</sub> hygroscopic characteristics in Kaohsiung City during winter. Even though there was no intensive filter sample collection during the studied period, the derived mean  $\kappa$  range under the specific assumption (solute density and ignorance of Kelvin effect) from AQB data was discussed for the range consistency compared to the results of available two winter campaigns for PM<sub>2.5</sub> and 2013 winter campaign for PM<sub>2.5-10</sub>. However, the temporal resolution for the derived hygroscopicity from IC data is higher than that derived from AQB data since the AQB analysis required a longer time period to cover a comprehensive range of RH to have the particle growth profile. The derived hygroscopicity then represents a mean value over a longer period. To clarify this approach, Section 3.3 (Lines 222-235): “A similar analysis for the winter of 2021 yielded a consistent  $\kappa$  range for PM<sub>2.5</sub>, as illustrated in Fig. S5. This consistency across distinct study periods indicates typical ambient PM<sub>2.5</sub> hygroscopic characteristics in Kaohsiung City during winter, which can be applied for further discussion with the AQB data. For coarse particles, the more significant variability in  $\kappa$  for PM<sub>2.5-10</sub> compared to PM<sub>2.5</sub> can be attributed to the significant fluctuations in the soluble composition of coarse particles, primarily driven by substantial quantities of thenardite (Na<sub>2</sub>SO<sub>4</sub>) and halite (NaCl) (Tang et al., 2019). ...The derived  $\kappa$  value for PM<sub>2.5</sub> from IC analysis (0.14-0.27) is consistent with that obtained from AQB analysis (~0.22), while the  $\kappa$  value for PM<sub>2.5-10</sub> from IC analysis (0.06-0.21) is relatively higher than that from AQB analysis (~0.09) (Table 1 and Fig. 4(a)). The  $\kappa$  differences between the IC and AQB analyses could be attributed to the spatial and temporal variations in aerosols, as well as the different campaign years and locations (~20 km apart, as shown in Fig. S1). These differences might also be influenced by technique uncertainties, such as ammonia and nitrate sampling evaporation during filter sampling (Hering and Cass, 1999; Chen et al., 2021), as well as OPC detection uncertainties and the required parameter assumption in the calculation. Overall, the derived  $\kappa$  values from the OPC data in AQB likely reflect the mean hygroscopicity of both integrated fine and coarse particles. “. Additionally, the corrected version of Fig. S5 is shown as:

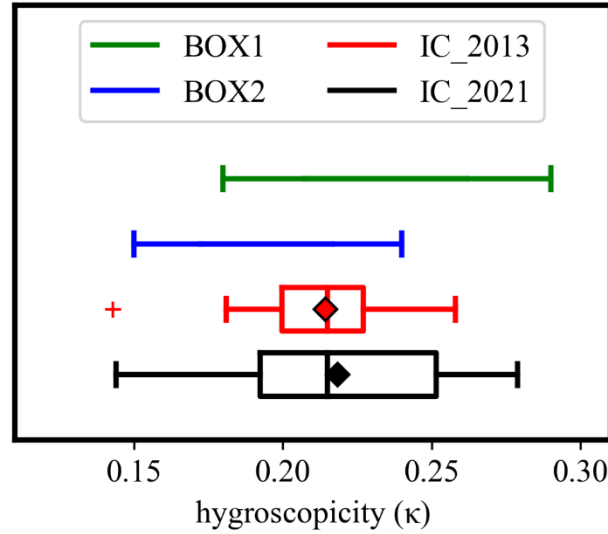


Figure S5: The hygroscopicity of PM<sub>2.5</sub> derived from AQB and IC data with an assumed particle density of 1.2 g cm<sup>-3</sup>. The IC\_2021 is from 2021 samples collected at the National Kaohsiung University of Science and Technology (22°46'22.4" N, 120°24'03.4" E) in Kaohsiung for the period of 8 – 18 December 2021 (diamond: mean value; outliers: < 1st quartile Q1-1.5 interquartile range (IQR) or > 3rd quartile Q3+1.5 IQR).

3) In Table 1, the hygroscopicity parameter kappa for PM<sub>2.5</sub> and PM<sub>2.5-10</sub> is smaller than the hygroscopicity parameter kappa for PM<sub>10</sub>, which is abnormal. PM<sub>10</sub> is the sum of PM<sub>2.5</sub> and PM<sub>2.5-10</sub>, and its hygroscopicity should be intermediate between the two.

A: The higher hygroscopicity of PM<sub>10</sub> than those of PM<sub>2.5</sub> and PM<sub>2.5-10</sub> is due to a significantly high portion PM<sub>2.5</sub> in PM<sub>10</sub> observed in AQB combined with the positive correlation between the derived sensitivity ( $\alpha$ ) and hygroscopicity ( $\kappa$ ), as shown in Eq. (3) for the ambient and dry PM mass concentration conversion.

$$M_{d,derived} = (\alpha \times M_{OPC}) \times \left[ \left( \frac{S\kappa}{1-S} \right) \times \frac{\rho_w}{\rho_d} + 1 \right]^{-1} \quad (3)$$

For a given  $M_{opc}$ , a higher  $\alpha$  would require a higher  $\kappa$  to have the same  $M_{d, derived}$ . Because the estimated  $\alpha$  for PM<sub>10</sub> is higher than that for PM<sub>2.5</sub>, a higher  $\kappa$  might be expected if PM<sub>2.5</sub> portion is dominant in PM<sub>10</sub>. This can be evaluated through the following calculation using an ideal system. The equation in the following shows the derived dry PM<sub>10</sub> concentration is the sum of the derived PM<sub>2.5</sub> and the derived PM<sub>2.5-10</sub> concentration.

$$\begin{aligned} (\alpha_{10} \times M_{10}) \times \left[ \left( \frac{S\kappa_{10}}{1-S} \right) \times \frac{\rho_w}{\rho_d} + 1 \right]^{-1} \\ = (\alpha_{2.5} \times M_{2.5}) \times \left[ \left( \frac{S\kappa_{2.5}}{1-S} \right) \times \frac{\rho_w}{\rho_d} + 1 \right]^{-1} + (\alpha_{2.5-10} \times M_{2.5-10}) \times \left[ \left( \frac{S\kappa_{2.5-10}}{1-S} \right) \times \frac{\rho_w}{\rho_d} + 1 \right]^{-1} \end{aligned}$$

where  $M$  is  $M_{opc}$  for different size ranges (indicated in the subscript). By assuming  $X$  as the ratio of  $M_{2.5-10}$  to  $M_{2.5}$  monitored by AQB, the relationship can be rewritten in the following:

$$\alpha_{10}(1 + X) \times \left[ \left( \frac{S\kappa_{10}}{1 - S} \right) \times \frac{\rho_w}{\rho_d} + 1 \right]^{-1} = \alpha_{2.5} \times \left[ \left( \frac{S\kappa_{2.5}}{1 - S} \right) \times \frac{\rho_w}{\rho_d} + 1 \right]^{-1} + (\alpha_{2.5-10} \times X) \times \left[ \left( \frac{S\kappa_{2.5-10}}{1 - S} \right) \times \frac{\rho_w}{\rho_d} + 1 \right]^{-1}$$

where the  $\rho_w$  and  $\rho_d$  are constants (assumed in this study), the sensitivity coefficients are given as  $\alpha_{2.5} = 1.26$ ,  $\alpha_{10} = 2.02$ , and  $\alpha_{2.5-10} = 12.37$  from Table 1, and hygroscopicity is given as a median value in derived results of PM<sub>2.5</sub> and PM<sub>2.5-10</sub> ( $\kappa_{2.5} = 0.24$ , and  $\kappa_{2.5-10} = 0.10$ ). The derived  $\kappa_{10}$  can be evaluated with a function of  $X$  and  $S$  in the following figure and is mainly affected by  $X$ . A higher  $\kappa_{10}$  than  $\kappa_{2.5}$  (0.24) is expected as  $X < 0.05$ , i.e., low  $M_{2.5-10}/M_{2.5}$ . The observed data from AQB has a higher probability of having  $X \sim 0.04$  with  $S \sim 0.8-0.9$  which leads to a higher derived  $\kappa_{10}$  than  $\kappa_{2.5}$  (0.24).

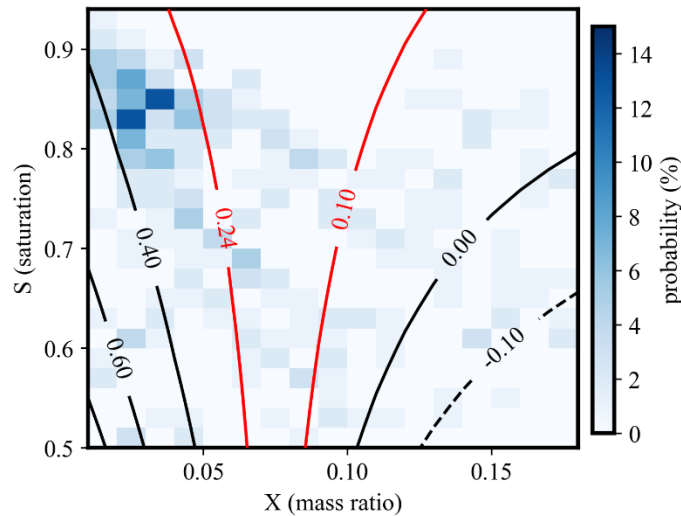


**Figure R2.** The distribution of the derived hygroscopicity of PM<sub>10</sub> in the condition of given sensitivity coefficients ( $\alpha_{2.5} = 1.26$ ,  $\alpha_{10} = 2.02$ , and  $\alpha_{2.5-10} = 12.37$ ) and hygroscopicity ( $\kappa_{2.5} = 0.24$ , and  $\kappa_{2.5-10} = 0.10$ ). The contour is the derived hygroscopicity of PM<sub>10</sub>, and the shading is the data point distribution of the AQB monitored data.

Overall, the estimated higher derived  $\kappa_{10}$  is possible to happen due to a significant amount of data points having a low portion PM<sub>2.5-10</sub> in PM<sub>10</sub> observed in AQB.

4) In Section 2.1, the author introduces the photo-ionization detector for monitoring VOCs, but in Figure 1 and subsequent manuscripts, the abbreviation used by the author is NMHC. These two abbreviations are not entirely equivalent.

The Alphasense PID-AH2 measures volatile organic compounds (VOCs) in the air using photoionization detection (PID), as stated in its datasheet. This device utilizes a lamp that emits high-energy UV photons. When a VOC molecule absorbs a photon, it generates electrically charged ions, creating an electric field. The detector then monitors the resulting current, which is proportional to the ambient VOC concentration. Notably, the PID-AH2 in this study uses a Krypton lamp with a photon energy of about 10.6 eV, capable of detecting some C2, and most C3, C4+ VOCs. In contrast, the Horiba APHA-360, a VOC gas analyzer used by TW-EPA, continuously analyzes THC, CH<sub>4</sub>, and non-CH<sub>4</sub> (NMHC) in ambient air using a flame ionization detector and cross flow modulation. Since the

ionization potential of methane is approximately 13.7 eV, the PID cannot detect its concentration, making NMHC the closest comparable data from TW-EPA for our purposes. Additionally, the sensitivity of the PID varies with the type of VOC detected; for example, toluene generates approximately twice the response of isobutylene. Consequently, as shown in Fig. 2(g), the sensor captures some peak NMHC concentrations, but not all temporal variations are detectable. To ensure consistency, the label in Fig.1 is revised as "VOCs". Furthermore, to avoid any potential confusion regarding the capabilities of the PID sensor, the following information is added in Section 2.1 (Lines 71-73): " The PID sensor, equipped with a Krypton lamp providing a photon energy of about 10.6 eV, cannot detect methane, which has a higher ionization potential of ~13.7 eV (Glockler, 1926). Therefore, the data of non-methane hydrocarbons (NMHC) from TW-EPA is more comparable to PID data in our analysis."

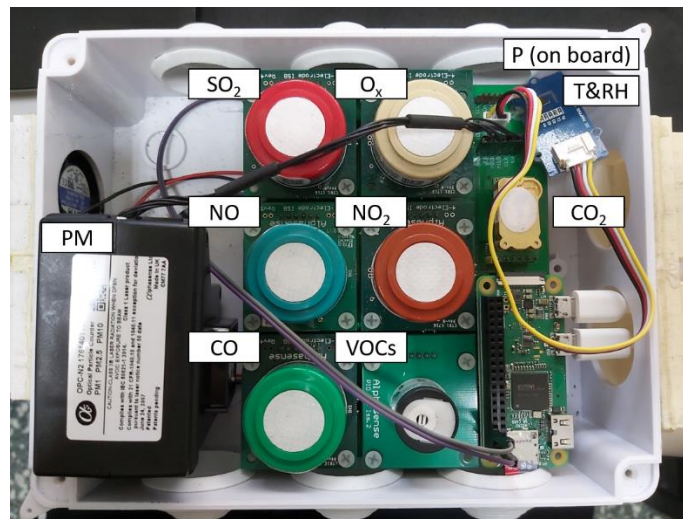


Figure 1: The design of the AQB system.